Available online at www.sciencedirect.com
SCIENCE DIRECT®
Biochimica et Biophysica Acta 1613 (2003) 87–100
BIOCHIMICA ET BIOPHYSICA ACTA
BBA
www.bba-direct.com

Interactions between glucosylceramide and galactosylceramide I^3 sulfate and microstructures formed

Awa Dicko[a,b], Yew M. Heng[c], Joan M. Boggs[a,b,*]

[a] Department of Structural Biology and Biochemistry, The Research Institute, The Hospital for Sick Children, Toronto, ON, Canada M5G 1X8
[b] Department of Laboratory Medicine and Pathobiology, University of Toronto, Toronto, ON, Canada M5G 1L57
[c] Department of Paediatric Laboratory Medicine, The Hospital for Sick Children, Toronto, ON, Canada M5G 1X8

Received 25 February 2003; received in revised form 1 May 2003; accepted 9 May 2003

Abstract

The monohexoside glycosphingolipids (GSLs), galactosylceramide (GalC), glucosylceramide (GluC), and their sulfated forms are abundant in cell membranes from a number of tissues. Carbohydrate–carbohydrate interactions between the head groups of some GSLs can occur across apposed membranes and may be involved in cell–cell interactions. In the present study, the ability of GluC to participate in trans interactions with galactosylceramide I^3 sulfate (CBS) was investigated by transmission electron microscopy (TEM) and Fourier transform infrared spectroscopy. Gaucher's spleen GluC had polymorphic phase behavior; in its metastable state, it formed large wrinkled vesicles. It transformed to a stable state via an intermediate state in which the surface of the vesicles consisted of narrow ribbons. In the stable state, the narrow ribbons split off from the surface to form membrane fragments and flat and helical ribbons. The strength of the intermolecular hydrogen bonding interactions between the carbonyls increased in the order metastable < intermediate < stable state. Aqueous dispersions of GluC and CBS were combined to allow trans carbohydrate–carbohydrate interaction across apposed bilayers, or the lipids were premixed in a solvent before hydration to allow lateral cis interactions. Premixed dispersions of NFA-GluC and CBS remained in the metastable state even when incubated under stable state conditions. When NFA-GluC dispersions were combined with CBS dispersions, they had a small effect on each other's amide groups in the metastable state. Furthermore, conversion of NFA-GluC to the stable state was inhibited, although it reached the intermediate state, suggesting that some degree of trans interaction between these two lipids occurred.

Keywords: Adhesion; Carbohydrate–carbohydrate interaction; Glycosphingolipid; Nanotube; Electron microscopy; FTIR spectroscopy

1. Introduction

The monohexoside glycosphingolipids (GSLs), galactosylceramide (GalC), glucosylceramide (GluC), and their sulfated forms are important in cell membranes from a number of tissues. In the myelin sheath about 20 mol% of the lipid consists of GalC and its sulfated derivative, cerebroside sulfate (CBS) [1]. In mutant mice lacking the enzyme required for galactolipid synthesis, UDP-galactose:ceramide galactosyltransferase (CGT), GluC is synthesized instead [2,3]. The myelin sheath is still formed but has defective function, stability, and interactions with the axon [4], indicating that GluC does not substitute completely for the functions of GalC. GluC is synthesized instead of GalC in the membranes which ensheath shrimp axons [5]. This sheath is multilayered like vertebrate myelin but less compacted. However, nerve conduction is faster than in other invertebrates such as earthworms which also have a multilayered sheath around nerve axons but lack GluC or other sphingolipids [6]. Schwann cells, which produce peripheral nervous system myelin, produce GluC instead of GalC until they start myelinating axons, when they switch to production of GalC and sulfated GalC [7].

Glycolipids are also very abundant in intestinal brush border membranes where they constitute 33% of the membrane lipid [8]. In these membranes, GluC is the major glycolipid and cholesterol sulfate is the major sulfated lipid [9]. Gastric and duodenal mucosa and kidney cell mem-

* Corresponding author. Department of Structural Biology and Biochemistry, The Research Institute, The Hospital for Sick Children, 555 University Ave., Toronto, ON, Canada M5G 1X8. Tel.: +1-416-813-5919; fax: +1-416-813-5022.
E-mail address: jmboggs@sickkids.ca (J.M. Boggs).

0005-2736/03/$ - see front matter © 2003 Elsevier B.V. All rights reserved.
doi:10.1016/S0005-2736(03)00141-X

branes contain significant amounts of GalC, GluC, and sulfated GalC [10,11]. Kidney cells also contain a small amount of sulfated GluC [12]. In the kidney of the CGT null mutant lacking galactolipids, GluC is increased slightly and more polar sulfoglycolipids such as sulfated lactosylceramide are increased two to three times, although sulfated GluC is not increased [13]. In polycystic kidney disease, the amount of GluC increases and the amount of sulfated GalC decreases [14]. The proportions of GluC, GalC, and sulfated GalC of MDCK cells vary with their ouabain resistance [15]. Uterine endometrium also contains GluC and sulfated GalC and the amount of the latter increases significantly from the follicular to the luteal phase [16,17]. Thus these monohexoside GSLs and their sulfated forms may play important roles in cell membranes.

Carbohydrate–carbohydrate interactions, sometimes mediated by divalent cations, between GSLs in apposed membranes may be involved in cell–cell interactions [18]. A trans interaction between GalC and CBS across apposed membranes has been detected by a liposome aggregation assay [19], binding of liposomes containing GalC to a CBS-coated surface [18], and by FTIR spectroscopy [20]. The interaction between these two lipids resulted in dehydration of the lipid head groups and a decrease in the intermolecular hydrogen bonding of the amide C=O of GalC. Ca^{2+}-mediated complex formation between these lipids in methanol was detected by mass spectrometry [21,22]. Addition of GalC/CBS-containing liposomes to oligodendrocytes in culture initiates transmembrane signal transmission, similar to the effect of anti-GalC antibodies [23], leading to the suggestion that a trans interaction may occur between these lipids in apposed membranes of compact myelin and participate in transmission of signals throughout the myelin sheath [24].

In order to determine the specificity of the GalC/CBS interaction, the interaction of CBS with GluC has also been investigated. Liposomal aggregation and mass spectrometry studies indicated that an interaction occurred but was weaker than that of GalC with CBS [18,19,22]. In the present work, FTIR spectroscopy was used to study the nature of the interaction between GluC and CBS. Aqueous dispersions of these lipids were combined to allow trans carbohydrate–carbohydrate interaction across apposed bilayers, or the lipids were premixed in a solvent before hydration to allow lateral cis interactions.

The thermodynamic behavior and the thermotropic properties of GluC, GalC, and CBS are similar and they form lamellar phases in the presence of water (reviewed in Ref. [25]). Differential scanning calorimetric (DSC), X-ray diffraction, and FTIR spectroscopic studies showed that aqueous dispersions of cerebrosides and sulfatide undergo complex polymorphic behavior [26–34]. On cooling, they transform from the liquid crystalline state to a metastable state which is then converted to more stable crystalline states. Previous transmission electron microscopy (TEM), freeze fracture electron microscopy, and atomic force microscopy studies showed that on cooling, aqueous dispersions of GalC and GluC form helical ribbons and nanotubular structures [35–40]. Their tendency to form helical ribbons increases in the presence of polar solvents [41,42] and CBS has also been found to form nanotubes in glycol [43]. However, the influence of the polymorphic phase behavior on the microstructures formed has not been previously reported. In the present study, TEM was used to investigate the microstructural changes associated with the transition from metastable to stable state of GluC and its mixtures with CBS.

2. Materials and methods

2.1. Materials

CBS from bovine brain was obtained from Matreya. The fatty acid composition of CBS reported by Matreya is 70% non-hydroxy fatty acids (NFA) and 30% hydroxy fatty acids (HFA), as reflected by the two spots observed on the TLC plate (not shown). Glucocerebroside from human Gaucher's Spleen (from Sigma), which contains predominantly non-hydroxy long chain saturated fatty acids, is designated NFA-GluC. It gave two spots by thin layer chromatography (TLC), a strong and a very light spot. Soybean glucocerebroside, which contains more than 95% α-hydroxypalmitic acid, is designated HFA-GluC and was purchased from Avanti Polar Lipids (Alabaster, AL). Deuterium oxide (99.9 at.%) was obtained from Sigma.

2.2. Sample preparation

The dry lipids were dissolved in chloroform/methanol 2:1. The solvent was evaporated under a stream of nitrogen and the lipids were dried under vacuum overnight. They were then dispersed in H_2O or D_2O by vortexing and heating the samples by dipping in boiling water several times, at a concentration of 1 mg/100 microliter for the pure lipids. For the mixtures, solutions of 1 mg of each lipid were mixed to give a final concentration of 2 mg/100 microliter. Four different samples were prepared: (i) CBS dispersion, (ii) GluC dispersion, (iii) aqueous CBS dispersion combined with aqueous GluC dispersion, (iv) premixed CBS/GluC dispersion prepared by combining the lipids in chloroform/methanol 2:1, evaporating the solvent and dispersing the dry lipid mixture in water. Ca^{2+} was not added as GalC and CBS were found to interact in the absence of Ca^{2+} if no other lipids were present [20]. For the metastable phase, the samples were cooled from 100 to 4 °C and kept at that temperature for 2 h before recording the spectra of the hydrated lipid suspensions at room temperature. In order to convert the sample to the stable phase after cooling to 4 °C, the hydrated lipid suspensions were incubated at room temperature or at −20 °C for varying periods of time as indicated in the text.

2.3. FTIR measurements

Spectra of hydrated lipids (in D_2O or H_2O) were recorded by spreading 10–20 microliter of the lipid suspensions between two CaF_2 windows, separated by a 15-micrometer Mylar spacer. Spectra of dried lipids were obtained by drying the aqueous lipid suspension (after incubation under metastable or stable state conditions) on a CaF_2 window with a stream of nitrogen, then placing under vacuum in a dessicator overnight at room temperature. This treatment did not affect conversion of the sample to the metastable or stable state. All the spectra were recorded at room temperature using a Bruker FTIR spectrometer, model IFS 48 equipped with a Germanium-coated KBR beam splitter and a DTGS detector. For each spectrum, 250 scans were co-added at 2 cm^{-1} resolution using triangular apodization. Data treatment was performed using SpectraCalc software (Galactic Industries Corp., Salem, NH). The second derivative (15 pts) of the spectrum was used to determine the frequency of the different components of unresolved bands. The Fourier deconvolution technique was used to resolve the amide bands using a narrowing parameter γ of 2.0 for NFA-GluC and CBS or 2.5 for HFA-GluC, and an apodization filter of 0.35 [44]. The frequencies of the methylene stretching vibration bands were determined as the midpoint at 80% of the height of each band [45]. Baseline correction was done and atmospheric water bands were subtracted from spectra, if necessary.

2.4. TEM measurements

Lipid suspensions cooled from 100 to 4 °C and incubated at 4 °C for 2 h for the metastable phase, or with subsequent incubation at room temperature or −20 °C for varying periods of time, as specified in the text and figure captions, were examined by TEM. An aliquot (5 microliter) of each lipid suspension was deposited on a formvar-coated 300-mesh copper grid, negatively stained with a 2% aqueous solution of phosphotungstic acid, and air-dried. The samples were analyzed in a JEM 1230 transmission electron microscope (JEOL USA, Inc.) operated at 80 kV. Digital images of 1024 × 1024 pixels were acquired with a CCD camera (AMT Advantage HR camera system, AMT, USA) attached to the microscope. Images were recorded at magnification ranges from 5000 × –100,000 × on the microscope settings.

3. Results

3.1. Glucocerebroside from Gaucher's spleen

Glucocerebroside from Gaucher's spleen, containing mostly non-hydroxy fatty acids (NFA-GluC), exhibits polymorphism depending on its thermal history. Fast cooling of dispersions of this lipid from the liquid-crystalline state to temperatures below the main transition temperature results in the formation of a metastable phase [27]. We found that it remained in the metastable phase at 4 °C for at least 2 h and routinely used the method of cooling from 100 to 4 °C followed by incubation at 4 °C for 2 h to obtain samples in the metastable phase. Other studies have reported that it can be converted to a more stable state by various thermal treatments, such as incubation of the sample at 70 °C for 5 min [30,33], or by prolonged incubation at −20 °C [32]. We found that incubation at −20 °C or at room temperature for more than 2 days gave a similar stable phase. However, incubation at 70 °C had no effect. Differences in fatty acid composition of our preparation may account for this as the fatty acid composition can significantly affect the kinetic barrier between the metastable and more stable phases [46]. Therefore, we routinely converted the sample to more stable phases by cooling from 100 to 4 °C and then incubating at room temperature for varying periods of time as specified below.

3.2. FTIR spectra of the metastable and stable states of NFA-GluC

The spectra of the amide I′ region of dry films of NFA-GluC, dried from a dispersion in D_2O in both the metastable and stable states, are shown in Fig. 1a. The spectrum of the metastable state was obtained after incubating the lipid dispersion at 4 °C for 2 h. The amide I′ band of NFA-GluC in the metastable state has its midpoint at 1628 cm^{-1}. The second derivative or deconvolution showed that the broad band is composed of two components at 1632 and 1616 cm^{-1} (Table 1). These bands are attributed to two populations of carbonyl groups with different strength of hydrogen bonding [47]. The presence of the band at 1616 cm^{-1} suggests a strong intermolecular interaction involving the carbonyl groups of a population of the lipid molecules.

When the lipid dispersions are then incubated at room temperature for 24–48 h, the amide band becomes narrower with its major component at 1628 cm^{-1} and a small band at 1612 cm^{-1} (Fig. 1b, Table 1). The intensity of the band at 1612 cm^{-1} increased with time at room temperature up to 48 h but did not shift in frequency (not shown). However, on subsequent incubation of the lipid dispersion at low (−20 °C) or room temperature for several days, a splitting of the amide I′ band occurs with a low frequency component emerging around 1606 cm^{-1} and a shift of the other band down to 1626 cm^{-1} (Fig. 1a). The bands at 1606 and 1626 cm^{-1} have been ascribed to the lipid in a stable state characteristic of a more rigid, tightly packed structure [33]. The state obtained after shorter-term incubation giving bands at 1628 and 1612 cm^{-1} has not been described previously. We suggest that it is an intermediate stable crystalline state. The strength of hydrogen bonding of the carbonyls of both populations of the lipid increases

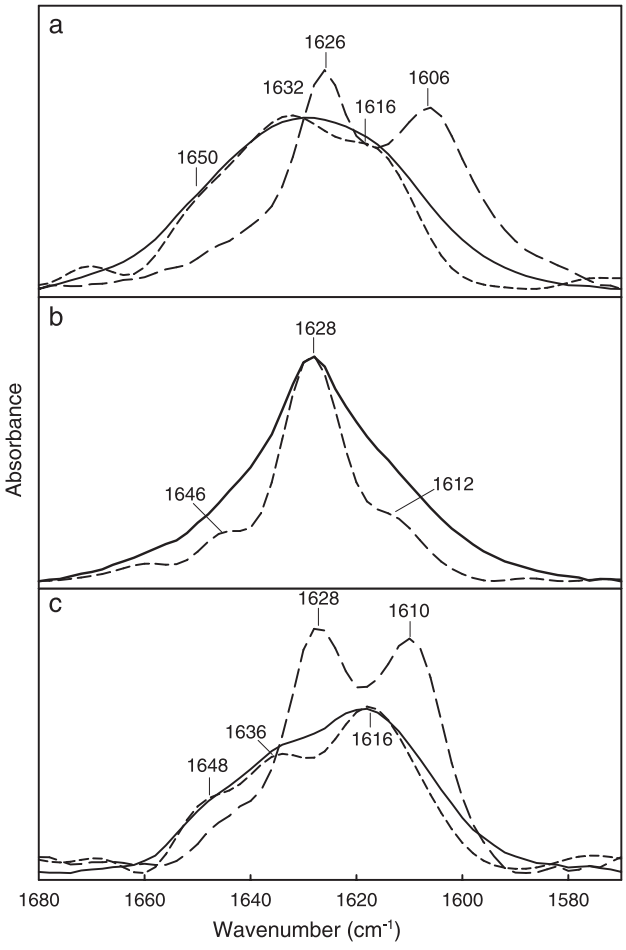

Fig. 1. FTIR spectra of amide I′region of NFA-GluC. (a) Metastable state, original spectrum (solid line) and corresponding deconvolved spectrum (short dashed line), plotted normalized to the same height. Stable state, original spectrum (dashed line). Dry films from a suspension in D_2O. (b) Intermediate state, original spectrum (solid line) and deconvolved spectrum (dashed line), plotted normalized to the same height. Dry film from a suspension in D_2O. (c) Metastable state, original spectrum (solid line) and corresponding deconvolved spectrum (short dashed line) plotted normalized to the same height. Stable state, original spectrum (long dashed line). Hydrated (D_2O) suspensions.

on going from the metastable to the intermediate to the stable state. An intermediate crystalline phase with hydrogen bonding strength between that of the metastable gel phase and the stable crystalline phase has also been observed for glucopyranosyldiacylglycerol [48]. Three crystalline phases of varying degrees of hydrogen bonding have been detected for NFA-GalC using FTIR spectroscopy [34].

The amide I′region of the hydrated (D_2O) suspension in the metastable state has a higher intensity of the low frequency component (1616 cm^{-1}) relative to higher frequency components (Fig. 1c). This indicates that in the presence of water, an increased percentage of the lipid carbonyl groups participate in moderate strength hydrogen bonds. The amide I′frequency of C=O hydrogen bonded to water molecules has previously been reported to appear around 1627–1632 cm^{-1} [49,50]. Thus, the band at 1616 cm^{-1} is probably due to hydrogen bonding of the C=O with hydrogen-donating groups in neighboring lipid molecules. The band at 1636 cm^{-1} is also unlikely to be due to hydrogen bonding with water since a similar band was present in the dehydrated sample. Thus the amide group is not hydrated in the metastable state in the presence of water.

The amide I′bands of the hydrated (D_2O) suspension in the stable state are somewhat increased in frequency to 1628 and 1610 cm^{-1} (Fig. 1c) relative to the dry film (Fig. 1a). Mueller and Blume [49] also observed two bands at about the same frequencies for GluC hydrated with D_2O, which were attributed to different types of intermolecular interactions between neighboring lipid molecules and between lipid and water. Although the band at 1628 cm^{-1} could be due to interactions of the C=O with water, we suggest that it is more likely due to interactions of the C=O in the stable state with neighboring lipid molecules,

Table 1
Frequencies of the amide I′bands from NFA-GluC

Sample	Amide I′		Amide II
	Dry films from D_2O	Hydrated films (D_2O)	Dry films from H_2O
NFA-GluC (metastable)	1650 (sh)	1648 (sh)	
	1632	1636	1546
	1616	1616	
NFA-GluC (Intermediate)	1646 (sh)		
	1628	–	–
	1612		
NFA-GluC (stable)	1644 (sh)	1646 (sh)	1544
	1626	1628	
	1606	1610	
CBS	1660 (sh)	1658 (sh)	
	1642	1642	1546
	1616	1620	
Combined Dispersions	1650 (sh)	1650 (sh)	
(metastable state conditions)	1634	1636	1546
	1616	1616	
Combined dispersions	1648 (sh)	1646 (sh)	
(stable state conditions)	1628	1628	1546
	1612	1610	
Premixed	1650 (sh)	1650 (sh)	
(metastable state conditions)	1638	1638	1548
	1616	1616	
Premixed	1650 (sh)	1646 (sh)	
(stable state conditions)	1638	1636	1548
	1616	1616	
Sum NFA-GluC + CBS	1650 (sh)	1642	1546
(metastable)	1638	1618	
	1616		
Sum NFA-GluC + CBS	1644 (sh)	1646 (sh)	
(stable)	1626	1628	1544
	1606	1610	

Most predominant spectral components are underlined. Second derivative of the bands were performed to determine their frequencies. sh = shoulder.

since a band appeared at nearly the same frequency for the dry film.

Spectra of dry films from dispersions in H_2O were also recorded in order to detect the amide II region. There was little change in amide II frequency on going from the metastable to the stable state (Table 1). The relatively high amide II frequency indicates involvement of the N-H in a linear intermolecular hydrogen bond, possibly with the

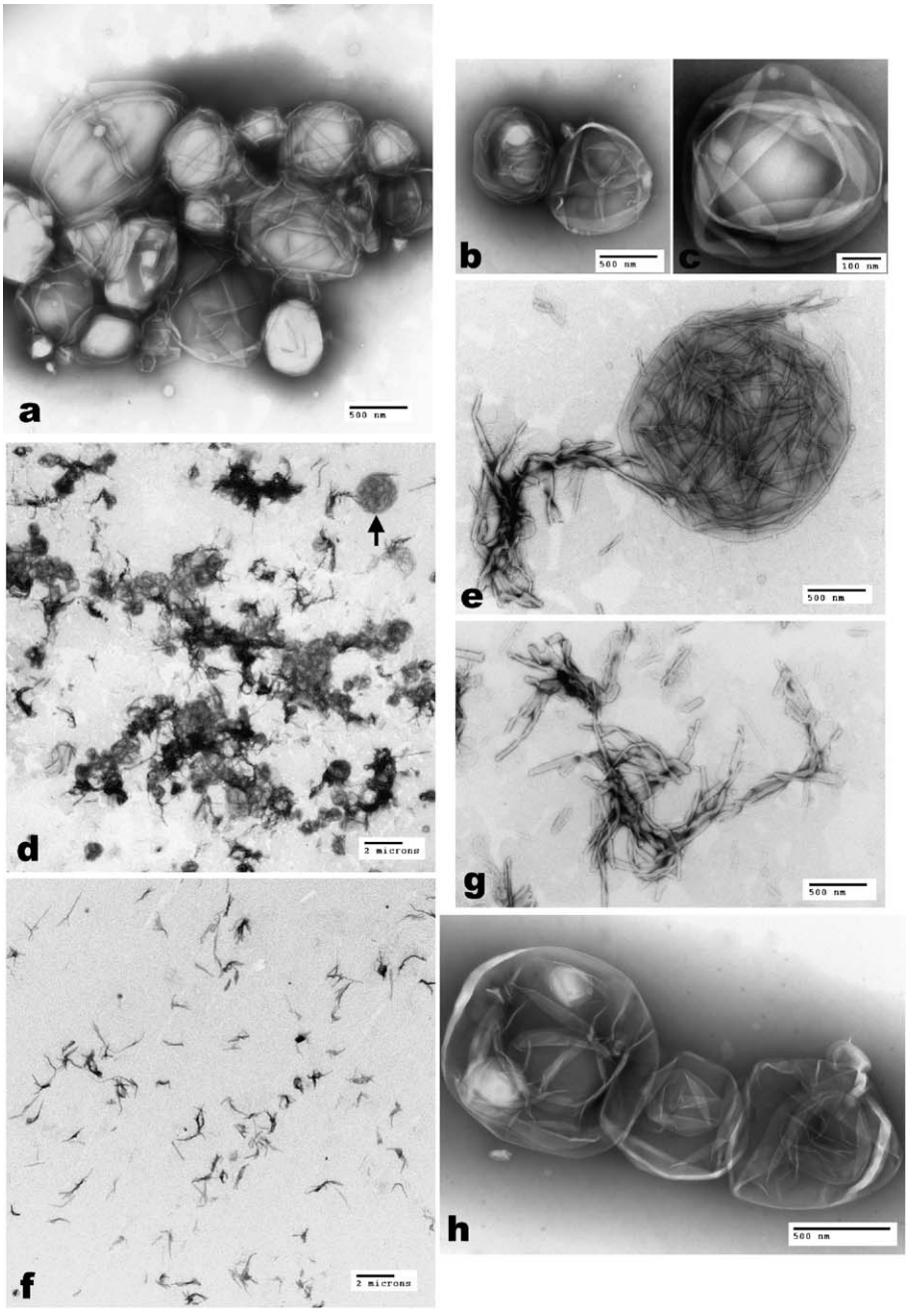

Fig. 2. Electron micrographs of negatively stained (a–g) NFA-GluC and (h) CBS, showing the polymorphic phase behavior of NFA-GluC and the microstructures formed by CBS. (a–c) Metastable state of NFA-GluC obtained after 2 h at 4 °C after cooling from above the phase transition temperature, showing vesicles with wrinkled and folded membrane layers. Some wide surface ribbons may also be present. (d, e) Intermediate state of NFA-GluC after subsequently incubating at room temperature for 48 h. Vesicle surfaces are almost completely broken up into ribbons, mostly narrower than any seen in the metastable state. Some of the ribbons have been shed from the vesicles. One vesicle with narrow surface ribbons indicated by an arrow in d is shown at higher magnification in e. (f, g) Stable state of NFA-GluC after incubating at room temperature for 2 weeks. The vesicles have mostly fragmented into flat or helical ribbons or short pieces of membrane strips. The ribbons are often wound around each other as shown at higher magnification in g. (h) CBS after cooling from above the phase transition temperature to 4 °C and incubation at 4 °C for 2 h. It forms wrinkled vesicles similar to those of the metastable state of NFA-GluC regardless of thermal history. It also forms some vesicles smaller than those shown. The degree of magnification is indicated by the bar which represents 500 nm in a, b, e, g and h, 100 nm in c, and 2 μm in d and f.

C=O of neighboring molecules, as found previously for NFA-GalC and NFA-CBS [33,51].

3.3. TEM of NFA-GluC in the metastable, intermediate, and stable states

TEM of negatively stained NFA-GluC shows that after cooling from the liquid crystalline phase, it forms large round structures resembling vesicles, with wrinkled or folded membrane layers (Fig. 2a–c). After incubation at room temperature for 1–2 days, the surface of the vesicles acquires a more detailed pattern which appears to consist of narrow strips and ribbon-like structures 50–100-nm wide (Fig. 2d and e). These narrow strips start to shed or split off from the surface. They then wind around each other and/or split off narrower ribbons (Fig. 2e). The narrow 50-nm ribbons are sometimes observed to be helical (Fig. 2e and g). After 2-week incubation, the large vesicles had mostly fragmented into membrane pieces and flat and helical ribbons (Fig. 2f), often still wound around each other (Fig. 2g). Formation of surface ribbons on the vesicles (Fig. 2d and e) coincided with the shift in amide I′ bands for the dry film from 1632 and 1616 cm^{-1} (Fig. 1a) to 1628 and 1612 cm^{-1} (Fig. 1b), while the conversion of these vesicles to shed membrane pieces and ribbons (Fig. 2f and g) correlated with the shift in amide I′ frequencies to 1626 and 1606 cm^{-1} (Fig. 1a). This indicates that the microstructures corresponding to the intermediate state are vesicles with surface ribbons, while those corresponding to the stable state are the split-off membrane pieces and ribbons. The wrinkled vesicles whose membranes have not yet split into narrow surface ribbons (Fig. 2a–c) contain the lipid in the metastable state. After taking a sample, which had been incubated at room temperature for 2 days, above the lipid phase transition temperature again and cooling back to room temperature, the membrane pieces and ribbons are gone, and wrinkled vesicles are again observed (not shown). Thus the process is reversible.

3.4. FTIR spectra and TEM of CBS

The amide I′band of a dry film of CBS from a dispersion in D_2O, cooled from 100 to 4 °C and incubated at 4 °C for 2 h, or at −20 °C for 10 days, is broad and centered near 1630 cm^{-1} (Fig. 3a). The deconvolved spectrum reveals two underlying components of similar intensity at 1642 and 1616 cm^{-1} (Fig. 3b, Table 1). The breadth of the amide I′ band and the fact that there are no bands below 1616 cm^{-1} indicates that the lipid is in a gel phase similar to the metastable phase of NFA-GluC and not a crystalline phase. The occurrence of metastable phase behavior has previously been reported for synthetic species of HFA and NFA-CBS using DSC [29], but not for the natural mixture used here [52]. The natural CBS mixture (containing both HFA- and NFA-CBS) did not convert to a more stable crystalline phase under our experimental conditions, although various incubation procedures and temperatures were tried. As observed above for NFA-GluC, hydration of CBS also causes an increase in the intensity of the low frequency amide I′ component relative to the higher frequency bands, but shifts it up to 1620 cm^{-1} (Fig. 3a and b). These changes indicate that the more strongly hydrogen-bonded carbonyl groups weaken somewhat in strength but increase in percentage relative to the more weakly hydrogen bonded population. However, the frequency at 1620 cm^{-1} suggests that they are involved in intermolecular hydrogen bonding with other lipid molecules rather than with water.

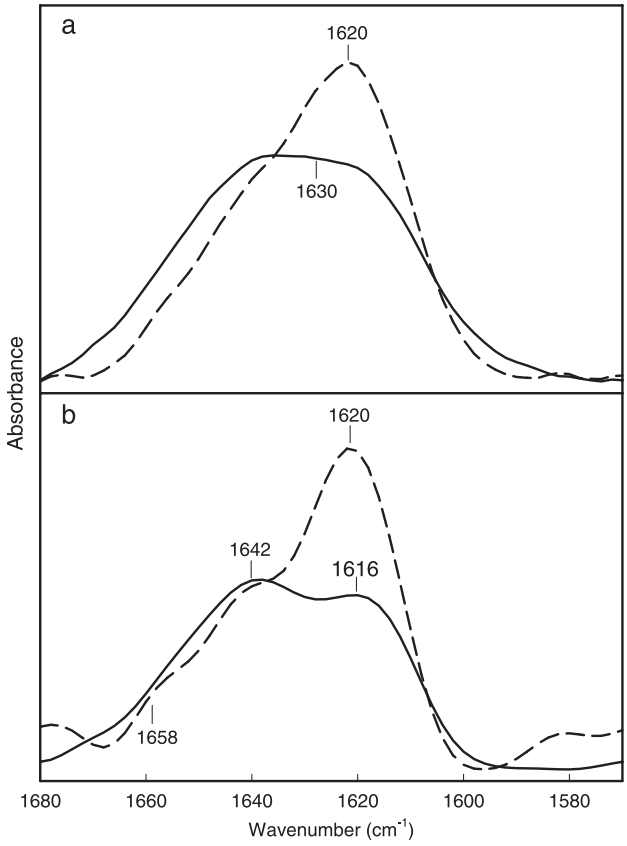

Fig. 3. FTIR spectra of amide I′region of CBS in the metastable state. Dry film from a suspension in D_2O (solid line), hydrated (D_2O) suspension (dashed line). (a) Original spectra; (b) corresponding deconvolved spectra.

The TEM pictures of CBS show vesicle-like structures of various sizes ranging from 40 to 900 nm (see Fig. 2h for larger ones). Similar to GluC in the metastable state, the large CBS structures also have wrinkled and folded membrane layers. No shed membrane pieces or ribbons were seen for CBS.

3.5. Interaction between NFA-GluC and CBS under metastable state conditions

NFA-GluC dispersions were combined with CBS dispersions to allow a trans GluC-CBS interaction to occur between apposed bilayers. Alternatively, NFA-GluC and

CBS were premixed in solvent before dispersion to allow lateral cis interactions within the same bilayer. Spectra of dry films of combined NFA-GluC and CBS dispersions and of a premixed NFA-GluC/CBS dispersion prepared by metastable state conditions (after 2-h incubation at 4 °C) are compared in Fig. 4a to the sum of the spectra of CBS and NFA-GluC obtained under metastable state conditions. The deconvolved spectra (Fig. 4b) of the premixed lipids and the sum of the NFA-GluC and CBS spectra show two bands at 1616 and 1638 cm^{-1} as well as a shoulder around 1650 cm^{-1} while these bands appear at 1616, 1634, and 1650 cm^{-1} for the combined dispersion (Table 1). The frequencies of hydrated films of the combined dispersions and the premixed lipids were close to those of dry films (Table 1). The similarity of the frequencies of the premixed GluC/CBS with those of the metastable states of the single lipids suggests that either the lateral cis interactions between the lipids in the mixture are of the same nature as in the single lipid dispersions or there are no cis interactions involving the carbonyl groups between NFA-GluC and CBS.

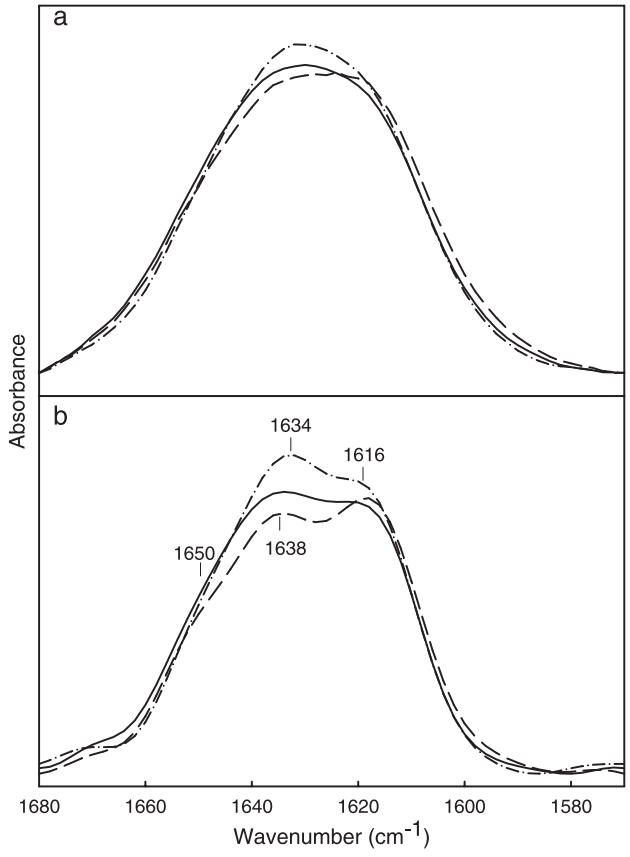

Fig. 4. FTIR spectra of amide I′ region of dry films of NFA-GluC/CBS combined and premixed dispersions under metastable state conditions. Combined dispersions (dot-dashed line); premixed dispersions (dashed line); sum of the spectra of NFA-GluC and CBS under metastable state conditions (solid line). (a) Original spectra; (b) corresponding deconvolved spectra. Samples were incubated at 4 °C for 2 h after cooling from the liquid crystalline phase.

When the lipid dispersions are combined, the small increase in intensity of the middle frequency component and its downward shift to 1634 cm^{-1} indicates that the C=O of a population of the lipid is involved in somewhat stronger hydrogen bonds than in the premixed or single lipids. This suggests that a trans interaction between NFA-GluC and CBS may occur when they are combined although it has only a small effect on the amide groups of the lipids under metastable state conditions. TEM of the combined dispersions under metastable state conditions showed wrinkled vesicles of varying sizes (Fig. 5a).

3.6. Interaction between NFA-GluC and CBS under stable state conditions

The spectra of dry films of premixed NFA-GluC/CBS and combined dispersions of NFA-GluC and CBS obtained after incubation of the dispersed samples at room temperature for several days are compared to the sum of the spectra of NFA-GluC and CBS obtained after similar incubation in Fig. 6a. Deconvolved spectra are shown in Fig. 6b. The spectrum of the amide I′ band of the premixed sample has two components around 1638 and 1616 cm^{-1} as well as a shoulder near 1650 cm^{-1} (Fig. 6b, Table 1). These frequencies are identical to those reported above for the premixed NFA-GluC/CBS sample in its metastable state. This suggests that formation of the stable state is prevented when the lipids are mixed in an organic solvent before the hydration step. This was confirmed by TEM which showed mostly small vesicles, about 100 nm in diameter (Fig. 5b), generally smaller than those observed for the metastable state of either GluC or CBS. A few larger wrinkled ones were also seen (not shown).

The major component of the spectrum of the combined dispersions under stable state conditions is at 1628 cm^{-1}, in addition to two bands of lower intensity around 1648 and 1612 cm^{-1} (Fig. 6a and b, Table 1). The spectral shape resembles that of the sum of the spectra of NFA-GluC and CBS obtained under stable state conditions, but the bands are all shifted to higher frequencies for the combined dispersions. In fact the frequencies are similar to those of the intermediate state of NFA-GluC. This indicates that formation of the stable state by NFA-GluC is prevented in the combined dispersions but the NFA-GluC is still able to go into the intermediate stable state in which intermolecular hydrogen bonding interactions of the C=O are weaker than for the stable state. This effect of CBS on NFA-GluC under stable state conditions indicates that a trans interaction occurs between the lipids. When a dispersion of NFA-GluC preconverted to the stable state is combined with a dispersion of CBS, the resulting spectrum is similar to that obtained by combining those dispersions in the metastable state and then incubating under stable state conditions (Fig. 6e and f). This indicates that not only does the presence of CBS vesicles prevent NFA-GluC from going into the stable state, it also causes

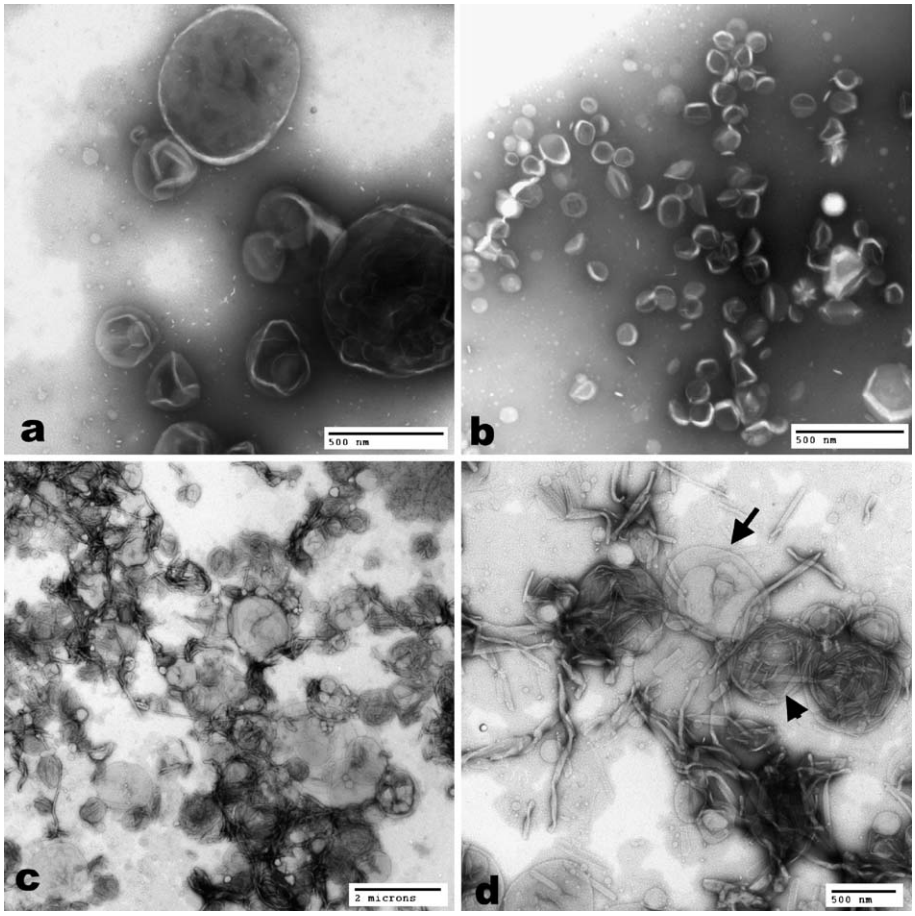

Fig. 5. Electron micrographs of negatively stained samples showing morphology of combined or premixed NFA-GluC/CBS dispersions. (a) Combined NFA-GluC and CBS dispersions incubated under metastable state conditions, for 2 h at 4 °C after cooling from above the phase transition temperature. Only wrinkled vesicles without surface ribbons or shed ribbons are seen. (b) Premixed NFA-GluC/CBS dispersions incubated under stable state conditions. The time of incubation had no effect on the morphology. (c, d) Combined NFA-GluC and CBS dispersions incubated under stable state conditions for 2 weeks at room temperature. Wrinkled vesicles typical of the metastable state of NFA-GluC and CBS (indicated by an arrow in d), vesicles with narrow surface ribbons typical of the intermediate state of NFA-GluC (indicated by an arrowhead in d), along with some shed membrane pieces and tangled ribbons are seen. The appearance resembles the intermediate state of NFA-GluC shown in Fig. 2d, although there are more vesicles lacking surface ribbons. The degree of magnification is indicated by the bar which represents 500 nm in a, b and d and 2 μm in c.

NFA-GluC to go back from the stable state to the intermediate state.

TEM of the combined dispersions of NFA-GluC and CBS under stable state conditions shows a mixture of wrinkled vesicles, vesicles with surface ribbons, and some unwound flat and helical ribbons (Fig. 5c and d). The wrinkled vesicles resemble those of CBS (arrow in Fig. 5d) and those with surface ribbons (arrowhead in Fig. 5d) resemble those of GluC in the intermediate state. However, GluC alone in the intermediate state also has some vesicles like those seen for CBS, so the type of structure seen by TEM in Fig. 5c and d does not unambiguously reveal the composition. TEM also does not reveal whether the two lipids interact, since a similar mixture of aggregated and tangled microstructures is seen for the intermediate state of NFA-GluC alone. However, it confirms that conversion of some of the lipid from the metastable to the intermediate state occurs in the combined dispersions.

Addition of a dispersion of CBS to a dispersion of NFA-GluC did not have any effect on the amide II frequency (Table 1). In contrast, the frequency of the amide II vibration of the premixed NFA-GluC/CBS is somewhat higher than that of the sum of the spectra of the individual lipids (Table 1). Since premixing the lipids did not affect the amide I frequency, the increase in the frequency of the amide II vibration is likely due to the formation of intermolecular hydrogen bonds between the N-H and oxygens of neighboring molecules other than the C=O, such as the sphingosine OH. These intermolecular interactions may occur between CBS and GluC.

In the hydrated state in D_2O, the amide I′ band of the combined dispersions, incubated for several days at room temperature, is composed of two main components near 1628 and 1610 cm^{-1} (Fig. 6c and d). The spectrum resembles that of the sum of the spectra of hydrated NFA-GluC and CBS in the stable state but is different from the spectrum of the premixed sample, which resembles the sum

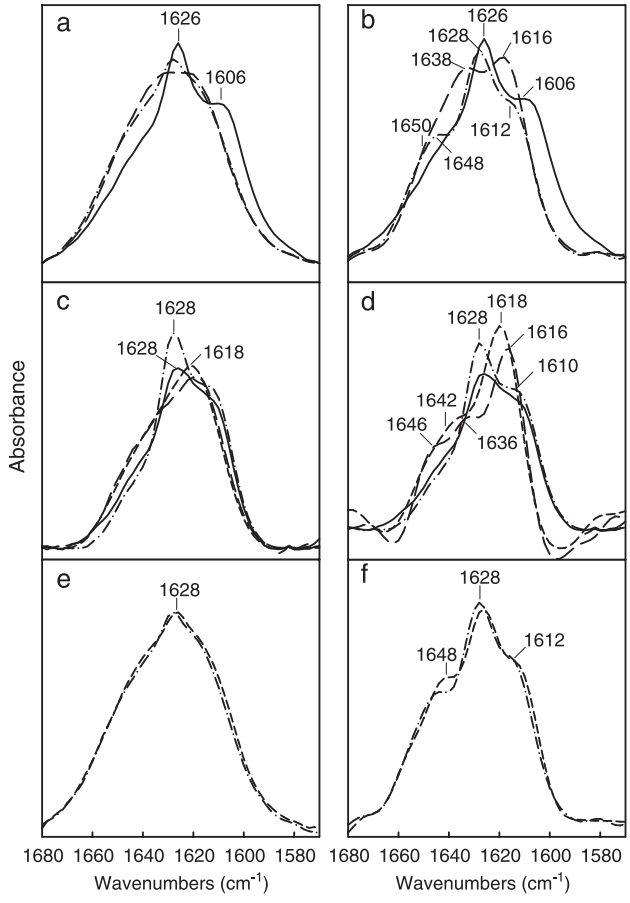

Fig. 6. (a, b, c, d) FTIR spectra of the amide I′ region of NFA-GluC/CBS combined and premixed dispersions, incubated under stable state conditions (room temperature for several days). Combined dispersions (dot-dashed line), premixed dispersions (long dashed line), sum of the spectra of NFA-GluC and CBS under stable state conditions (solid line). (a) Original spectra, dry films from a suspension in D_2O. (b) Deconvolved spectra of the combined dispersions and premixed dispersions from (a); sum of the spectra of NFA-GluC and CBS under stable state conditions is not deconvolved. Spectra are plotted out at similar heights. (c) Hydrated (D_2O) suspension. The sum of the spectra of NFA-GluC and CBS under metastable state conditions is also shown in (c) (short dashed line). (d) Deconvolved spectra of the premixed dispersions and of the sum of the spectra of NFA-GluC and CBS under metastable state conditions, from (c); spectra of the combined dispersions and sum of the spectra of NFA-GluC and CBS under stable state conditions are not deconvolved. (e, f) Spectrum of dry film of NFA-GluC dispersion preconverted to the stable state and combined with CBS dispersion (short dashed line), compared to the spectrum of the combined dispersions incubated under stable state conditions after combining (dot-dashed line). The latter is identical to the dot-dashed line in (a). (e) Original spectra; (f) corresponding deconvolved spectra.

of the spectra of the hydrated lipids in their metastable state. This indicates that in the hydrated combined dispersions, the two lipids behave as in the single lipid dispersions and the stable state still occurs. The similarity of the spectra of the combined dispersions with that of the sum of the stable state spectra indicates that either the lipids do not interact by trans interactions when hydrated, or their trans interactions have no effect on their carbonyl groups.

3.7. Sulfate region

The antisymmetric stretching vibration of the sulfate group gives a large band between 1350 and 1180 cm^{-1} that overlaps with the methylene wagging progression. For dried samples, the sulfate band has its maximum around 1214 cm^{-1} for pure CBS, the premixed NFA-GluC/CBS, and the combined NFA-GluC and CBS dispersions (not shown). This suggests that the sulfate group is not affected by the addition of NFA-GluC to CBS. The second derivative spectra of the hydrated samples reveal that the sulfate band appears at nearly the same frequency as for the dry samples.

3.8. FTIR spectra of soybean glucocerebroside (HFA-GluC)

The amide I′ band of a dry film of soy GluC, containing mainly hydroxy fatty acids (HFA-GluC), cooled from above the phase transition temperature to room temperature, has its midpoint at 1636 cm^{-1} (Fig. 7a). Lynch et al. [31] reported that GluC isolated from the leaves of winter rye (95% HFA-GluC) forms a metastable phase on cooling from the liquid crystalline phase, which converted to a stable phase on holding at 0 °C for an hour. Therefore, dispersions of soy HFA-GluC, cooled from above the phase transition temperature, were incubated for 1–2 h at 4 °C, or 10 days at −20 °C, or 1–4 days at room temperature before recording the spectrum at room temperature. Under all experimental conditions, the spectra showed broad amide I′ bands centered at 1636 cm^{-1} similar to that described above, indicating that soy HFA-GluC does not form a more stable state under these conditions. A possible reason for the different behavior of the HFA-GluC from the two sources may be the significant differences in the ceramide composition [31,53].

Deconvolution of the broad band centered at 1636 cm^{-1} revealed two major components near 1644 and 1628 cm^{-1} as well as shoulders near 1612 and 1660 cm^{-1} (Fig. 1a, Table 2). The frequencies of the major components are higher than those of the metastable state of the NFA form, suggesting that the C=O group is more weakly hydrogen-bonded in the HFA species. A similar observation was previously made for NFA- and HFA-CBS [51] and for the stable crystalline states of NFA- and HFA-GalC [34]. However, in the metastable phase of GalC, the C=O of the HFA species was more strongly hydrogen-bonded than that of the NFA species [33,34].

The frequency of the amide II band of HFA-GluC is significantly lower than that of NFA-GluC (Tables 1 and 2). A similar difference in frequency between the HFA and NFA species was previously observed for CBS [51], GalC [33], and ceramide [54]. The low amide II frequency for HFA-GluC indicates that its N-H probably participates in a bifurcated intramolecular hydrogen bond with the fatty acid α-hydroxyl group and the oxygen of the glycosidic linkage, as shown for HFA-GalC in crystal form [55].

3.9. Interaction between HFA-GluC and CBS

The amide I′ spectra of dry films of premixed HFA-GluC/CBS and the combined dispersions of HFA-GluC and CBS are similar and resemble that of the sum of the spectra of the two lipids (Fig. 7b). However, deconvolution shows that the lowest frequency band of the premixed sample is shifted upward from that in the combined dispersions or the sum (Fig. 7c), indicating a weakening of the C=O hydrogen bonds when CBS and HFA-GluC are premixed. In the combined dispersions, the two lipids either do not interact by trans interactions, or their trans interactions result in no effect on the carbonyl groups of either lipid.

The amide II frequency of the premixed and combined dispersions is similar to that of the summed spectra (Table 2). This indicates that the intramolecular hydrogen bonds that the N-H of HFA-GluC forms with the other oxygen molecules are not disrupted by the presence of CBS in either cis or trans interaction. The strength of the intermolecular hydrogen bonds which the N-H of CBS (NFA species) participates in is also not affected by mixing with HFA-GluC, although they may take place between CBS and HFA-GluC in the mixture rather than solely between CBS molecules. However, since intermolecular hydrogen bonds of the C=O of HFA-GluC and/or CBS are weakened when mixed together as noted above, intermolecular hydrogen bonds of the N-H of CBS probably do not involve the C=O of HFA-GluC, but some other oxygen.

Table 2
Frequencies of the amide I′band from HFA-GluC

Sample	Amide I′	Amide II
	Dry films from D_2O	Dry films from H_2O
HFA-GluC	1660 (sh)	
	1644	
	1628	1534
	1612	
CBS	1660 (sh)	
	1642	1546
	1616	
Combined Dispersions	1660 (sh)	
	1644	1538
	1624	
	1616	
Premixed	1650	
	1638	
	1620	1538
Sum (HFA-GluC + CBS)	1660 (sh)	
	1644	
	1624	1538
	1614	

Most predominant spectral components are underlined. Second derivative of the bands were performed to determine their frequencies. sh = shoulder.

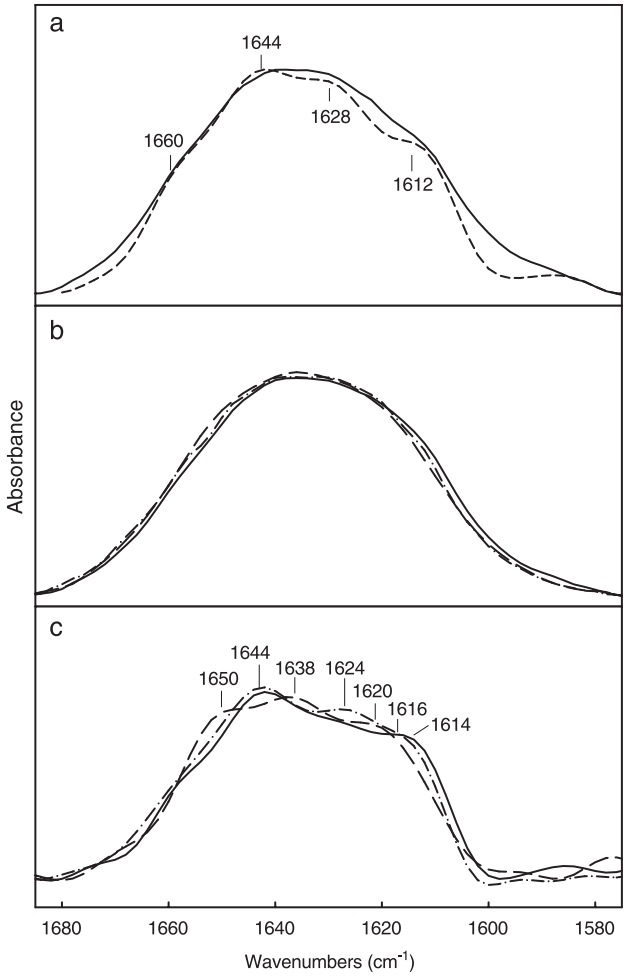

Fig. 7. (a) FTIR spectrum of the amide I′region of a dry film of HFA-GluC (solid line) and corresponding deconvolved spectrum (short dashed line), plotted normalized to the same height; (b, c) FTIR spectra of dry films of the combined dispersions (dot-dashed line), premixed dispersions (dashed line), and sum of the spectra of HFA-GluC and CBS (solid line). Original spectra are shown in b and deconvolved spectra in c.

3.10. Hydrocarbon chain region

The antisymmetric and symmetric methylene stretching vibrations are sensitive to the conformation of the acyl chains [56]. The frequency of the CH_2 symmetric vibration of NFA-GluC in the stable state is 2849 cm^{-1}, slightly lower than in the metastable state (~ 2850 cm^{-1}), consistent with the formation of a more rigid structure in the former. This contrasts with the reported behavior of NFA-GalC, for which the metastable phase had a much lower CH_2 symmetric stretching vibration than the stable phase [34]. This may be due to differences in fatty acid composition, as NFA-GalC has a high percentage of 24:1. The band resulting from the scissoring CH_2 mode in both the metastable and stable states of NFA-GluC is composed of mainly one band at 1468 cm^{-1} and a shoulder near 1452 cm^{-1} (not shown), suggesting a hexagonal chain packing in both states [48,54].

4. Discussion

GluC and CBS have high gel to liquid crystalline phase transition temperatures [25,52,57]. Consequently, at physiological temperatures, they are in an ordered state, as reflected by the low frequency of the methylene stretching vibration bands. The NFA-GluC from Gaucher's spleen used in the present study contains mostly saturated long chain fatty acids [57] while the soy HFA-GluC contains mostly hydroxy-palmitic acid [53].

In the present study, the polymorphism exhibited by GluC and its interaction with CBS have been monitored by FTIR spectroscopy and TEM. NFA-GluC was investigated in both its metastable and stable states and shown to also form an intermediate stable state. Freire et al. [27] have proposed that the conversion of NFA-GluC to the stable state does not involve a major rearrangement of the hydrocarbon chains. Indeed, the present results show that there is not much variation of the frequency of the methylene vibrational and scissoring modes on going from the metastable to the stable state. Furthermore, in their study of synthetic C16:0 GalC and GluC, Saxena et al. [32] have reported that both the metastable and stable states of these lipids have an ordered crystalline packing arrangement and the transition to the stable state is accompanied by a change in the chain packing mode. A reorientation of the acyl chains would not necessarily be reflected in the frequency of the methylene stretching vibration. However, the FTIR results provide new information in revealing an intermediate stable state and in showing that the strength of hydrogen bonding of the C=O increased in the order metastable state < intermediate state < stable state. Similar results were obtained by Bou Khalil et al. [34] for the three phases of NFA-GalC.

TEM showed that different microstructures were formed in the three states of NFA-GluC. Both NFA-GluC and CBS formed wrinkled vesicles in their metastable states while the vesicles of NFA-GluC acquired surface ribbons in the intermediate state. These ribbons split off from the vesicles in the stable state and were both flat and helical and often wound around each other. Similar structures as those shown for the intermediate and stable states have been previously observed for GluC purified from Gaucher cells [36] and for GalC [37], but the metastable state of GluC has not previously been characterized nor has there been any previous correlation of microstructure with the thermal history of the sample or FTIR spectra.

The ribbons are probably lamellar since they have been observed to form uni- and multilamellar tubules under some conditions [36,37]. The tubules are more often seen by freeze fracture and by atomic force microscopy, or by negative staining TEM when dried from polar solvents, while the ribbons are more often seen by negative-staining TEM when dried from water [36,37,40–43]. The microstructure formed also depends on the acyl chain length and degree of unsaturation [36,37]. We did not observe any structures which were clearly tubules. Dehydration for negative staining TEM may stabilize the flat and helical ribbons. In the ribbons, the lipid acyl chains will be exposed to water at the edges of the lamellae. They can be sequestered from water by formation of tubules from the helical ribbons [39,58].

The chirality inherent to cerebrosides and other lipids is believed to cause this behavior. Chiral diacetylenic lipids also form helical ribbons and tubules in the gel state [59]. However, in the liquid crystalline state they form lamellae in which the packing is no longer chiral [58]. When the lipid undergoes the transition to the gel phase, tilting of the lipid and chiral packing occur, leading to stripe-like domains of different molecular orientation in the lipid bilayer [39,58]. Our TEM and FTIR results indicate that this change in packing correlates with the transition of the metastable state to the intermediate stable state and is accompanied by stronger intermolecular hydrogen bonding of the carbonyl groups. These organized domains can then break off to form flat membrane pieces and ribbons. This change in structure correlates with the transition of the intermediate state to the stable state in which intermolecular hydrogen bonding of the carbonyl groups increases further. The increased chiral packing on going from the metastable to the intermediate to the stable state may allow the increased intermolecular hydrogen bonding between the carbonyls and other groups in neighboring lipid molecules. There are kinetic barriers to the organized chiral packing of the intermediate and stable states and splitting off of ribbons from the vesicles. When the split-off ribbons are sufficiently narrow, the twist from neighbor to neighbor causes them to become helical. In the presence of water, these can then form tubules and can be detected by freeze fracture or atomic force microscopy where the sample is kept hydrated, or by negative staining TEM when the sample has been dried from a polar solvent, such as glycol.

Previous X-ray diffraction studies have shown that in their metastable states, the head groups of NFA-GluC and GalC are dehydrated [28,32]. Rehydration of the polar head group is believed to occur on formation of the stable state. The hydration state of the head group of GluC in different states could not be determined from our FTIR results, although the low amide I′ frequency indicates that the carbonyl of the metastable state is unlikely to be hydrated. In the stable state, amide I′ frequencies were similar for dry and hydrated films, indicating that hydrogen bonded C=O groups were more likely interacting with neighboring lipid molecules than with water in that state also. The TEM results showed that in the metastable state, NFA-GluC formed multilayered vesicles. If water is excluded from between the bilayers, as indicated by the X-ray diffraction results, then the head groups would be sequestered from water. When the bilayers split into ribbons in the intermediate state, this would allow infiltration of water, exposing the head groups and acyl chains on the ribbon edges to water. Unwinding of the ribbons would allow them to form

helical tubules which would sequester the fatty acid chains from water but leave the head groups exposed to water. Although we did not observe the formation of tubules from the helical ribbons in the dry state used for negative staining, tubules have been observed by others by freeze fracture for Gaucher's spleen NFA-GluC [36].

CBS was also observed by TEM to form wrinkled vesicles. Saxena et al. [60] have also observed limited hydration and lack of swelling with addition of increasing amounts of water for synthetic C16:0-CBS by X-ray diffraction. Thus, the CBS vesicles may also exclude water.

In the metastable, intermediate, and stable states, the amide I band of NFA-GluC has two or more distinct components. A splitting of the amide modes (both I and II) was observed by Moore et al. [54] for NFA ceramide, due to the intermolecular coupling of the amide groups vibrational modes. This interpretation is ruled out for NFA-GluC in the stable state because the amide II band has only one component. Steric hindrance by the pyranose ring in the glycolipid may prevent such close packing. Furthermore, the amide groups of GluC probably interact with other OH groups, preventing splitting due to intermolecular coupling, as proposed by Moore et al. [54] for HFA ceramide. Thus, the two major components of the amide I band of GluC are likely due to two different populations of carbonyl groups. Two or more populations of hydrogen-bonded carbonyls have been consistently observed for monohexoside GSLs such as GalC, GluC, and CBS, even though there is only one carbonyl group in the molecule [33,34,49–51]. The microstructures seen by TEM may explain this since they indicate the lipid molecules must experience different environments at the edges of the lamellar ribbons compared to the interior of the ribbons. The outer lamella of the metastable phase vesicles will also be exposed to a different environment than the inner lamellae. These different environments could lead to differences in molecular packing and/or hydrogen bonding interactions of the amide group.

Both FTIR and TEM results indicate that premixing CBS and NFA-GluC before their hydration prevents the formation of the intermediate or stable states. The mixture formed predominantly smaller vesicles than those formed by GluC alone in the metastable state and they persisted under stable state conditions. The absence of ribbons for the premixed sample under stable state conditions shows that GluC did not phase separate from CBS since the microstructure of the mixture is significantly different from that formed by either lipid alone. Although there was no effect of the interaction on intermolecular hydrogen bonding interactions of the C=O groups, there was a small effect on the N-H groups. When HFA-GluC was mixed with CBS, there was no effect on intramolecular hydrogen bonding interactions of the N-H group, but intermolecular hydrogen bonding interactions of the C=O were weakened.

When CBS and NFA-GluC dispersions were combined in the metastable state, intermolecular hydrogen bonding interactions of the C=O were strengthened somewhat for dry films, suggesting that a trans interaction occurred. FTIR and TEM results showed that formation of a stable state was prevented when CBS and NFA-GluC dispersions were combined, in support of this conclusion. However, unlike the premixed dispersions, the combined dispersions were able to go into the intermediate state when incubated under stable state conditions. Interaction of the NFA-GluC vesicles with CBS vesicles may have prevented splitting off of the surface ribbons from the GluC vesicles. Interestingly, when GluC was preconverted to the stable state and combined with CBS dispersions, the FTIR results indicated that the intermolecular hydrogen bonding interactions of NFA-GluC became like that in its intermediate state. Possibly the split-off ribbons of NFA-GluC in its stable state bound to the CBS vesicles; this might result in a similar degree of hydrogen bonding as in the intermediate state of NFA-GluC alone. In the presence of excess water, CBS and GalC had no effect on their amide groups when the dispersions were combined and incubated under stable state conditions, suggesting that the presence of excess water may have inhibited trans interactions between the lipids.

When CBS dispersions were added to HFA-GluC dispersions, there was no effect on the amide I and II bands even in the dry state. Either a trans interaction did not affect the hydrogen bonding interactions of the amide groups or there was no trans interaction between HFA-GluC and CBS. When these lipids were premixed, the intermolecular hydrogen bonding of the C=O group was weakened. There was no effect on intramolecular interactions of the N-H group. Intramolecular interactions between the N-H and the glycosidic oxygen of HFA-GalC and HFA-CBS cause the sugar head group to be bent over parallel to the bilayer, while in the NFA species of CBS, it may be extended into the aqueous phase [51,55]. NMR showed that the sugar head group of NFA-GluC is also extended into the aqueous phase [61]. Our FTIR results on HFA-GluC show that the N-H is involved in an intramolecular hydrogen bond which should stabilize the bent-over conformation as for HFA-GalC and HFA-CBS. These differences in conformation may account for differences in the interaction of NFA- and HFA-GluC with CBS.

Thus, as indicated by mass spectrometry [22], a trans interaction between NFA-GluC and CBS can occur. Such interactions might be involved in cell–cell interactions in the intestinal brush border, kidney, and uterine endometrium where both of these lipids occur.

Acknowledgements

This work was supported by a grant from the Canadian Institutes for Health Research to JMB and an Astra Zeneca/CIHR/Multiple Sclerosis Society of Canada post-doctoral fellowship to AD.

References

[1] W.T. Norton, Isolation and characterization of myelin, in: M.P. Morell (Ed.), Plenum, New York, 1977, pp. 161–199.
[2] T. Coetzee, N. Fujita, J. Dupree, R. Shi, A. Blight, K. Suzuki, K. Suzuki, B. Popko, Myelination in the absence of galactocerebroside and sulfatide: normal structure with abnormal function and regional instability, Cell 86 (1996) 209–219.
[3] A. Bosio, E. Binczek, W. Stoffel, Functional breakdown of the lipid bilayer of the myelin membrane in central and peripheral nervous system by disrupted galactocerebroside synthesis, Proc. Natl. Acad. Sci. U. S. A. 93 (1996) 13280–13285.
[4] B. Popko, Myelin galactolipids: mediators of axon–glial interactions? Glia 29 (2000) 149–153.
[5] Y. Kishimoto, Phylogenetic development of myelin glycosphingolipids, Chem. Phys. Lipids 42 (1986) 117–128.
[6] N. Okamura, H. Yamaguchi, M. Stoskopf, Y. Kishimoto, T. Saida, Isolation and characterization of multilayered sheath membrane rich in glucocerebroside from shrimp ventral nerve, J. Neurochem. 47 (1986) 1111–1116.
[7] J.K. Yao, A.J. Windebank, J.F. Poduslo, J.E. Yoshino, Axonal regulation of Schwann cell glycolipid biosynthesis, Neurochem. Res. 15 (1990) 279–282.
[8] H. Hauser, K. Howell, R.M.C. Dawson, D.E. Bowyer, Rabbit small intestinal brush border membrane preparation and lipid composition, Biochim. Biophys. Acta 602 (1980) 567–577.
[9] G.C. Hansson, The subcellular localization of the glycosphingolipids in the epithelial cells of rat small intestine, Biochim. Biophys. Acta 733 (1983) 295–299.
[10] H. Natomi, T. Saitoh, K. Sugano, M. Iwamori, M. Fukayama, Y. Nagai, Systematic analysis of glycosphingolipids in the human gastrointestinal tract: Enrichment of sulfatides with hydroxylated longer-chain fatty acids in the gastric and duodenal mucosa, Lipids 28 (1993) 737–742.
[11] J.A. Shayman, N.S. Radin, Structure and function of renal glycosphingolipids, Am. J. Physiol. 260 (1991) 291–302.
[12] N. Iida, T. Toida, Y. Kushi, S. Handa, P. Fredman, L. Svennerholm, I. Ishizuka, A sulfated glucosylceramide from rat kidney, J. Biol. Chem. 264 (1989) 5974–5980.
[13] K. Tadano-Aritomi, T. Hikita, H. Fujimoto, K. Suzuki, K. Motegi, I. Ishizuka, Kidney lipids in galactosylceramide synthase-deficient mice: absence of galactosylsulfatide and compensatory increase in more polar sulfoglycolipids, J. Lipid Res. 41 (2000) 1237–1243.
[14] G.D. Deshmukh, N.S. Radin, V.H. Gattone II, J.A. Shayman, Abnormalities of glycosphingolipid, sulfatide, and ceramide in the polycystic (cpk/cpk) mouse, J. Lipid Res. 35 (1994) 1611–1618.
[15] Y. Niimura, I. Ishizuka, Glycosphingolipid composition of a renal cell line (MDCK) and its ouabain-resistant mutant, J. Biochem. 100 (1986) 825–835.
[16] K. Kubushiro, K. Kojima, M. Mikami, S. Nozawa, R. Iizuka, M. Iwamori, Y. Nagai, Menstrual cycle-associated alteration of sulfogalactosylceramide in human uterine endometrium: Possible induction of glycolipid sulfation by sex steroid hormones, Arch. Biochem. Biophys. 268 (1989) 129–136.
[17] K. Takamatsu, K. Kamei, K. Kubushiro, K. Kiguchi, S. Nozawa, M. Iwamori, Luteal phase-characteristic induction of I_3SO_3-GalCer in human cervical epithelia and uterine endometria, and follicular phase-characteristic formation of a ganglioside-derived negative charge gradient in different regions of fallopian tubes, Biochim. Biophys. Acta 1170 (1993) 232–236.
[18] S.-I. Hakomori, Carbohydrate–carbohydrate interaction as an initial step in cell recognition, Pure Appl. Chem. 63 (1991) 473–482.
[19] R.J. Stewart, J.M. Boggs, A carbohydrate–carbohydrate interaction between galactosylceramide-containing liposomes and cerebroside sulfate-containing liposomes: dependence on the glycolipid ceramide composition, Biochemistry 32 (1993) 10666–10674.
[20] J.M. Boggs, A. Menikh, G. Rangaraj, Trans interactions between galactosylceramide and cerebroside sulfate across apposed bilayers, Biophys. J. 78 (2000) 874–885.
[21] K.M. Koshy, J.M. Boggs, Investigation of the calcium-mediated association between the carbohydrate head groups of galactosylceramide and galactosylceramide I-3 sulfate by electrospray ionization mass spectrometry, J. Biol. Chem. 271 (1996) 3496–3499.
[22] K.M. Koshy, J. Wang, J.M. Boggs, Divalent cation-mediated interaction between cerebroside sulfate and cerebrosides: an investigation of the effect of structural variations of lipids by electrospray ionization mass spectrometry, Biophys. J. 77 (1999) 306–318.
[23] C.A. Dyer, J.A. Benjamins, Glycolipids and transmembrane signaling: antibodies to galactocerebroside cause an influx of calcium in oligodendrocytes, J. Cell Biol. 111 (1990) 625–633.
[24] J.M. Boggs, H. Wang, Effect of liposomes containing cerebroside and cerebroside sulfate on cytoskeleton of cultured oligodendrocytes, J. Neurosci. Res. 66 (2001) 242–253.
[25] R. Koynova, M. Caffrey, Phases and phase transitions of the sphingolipids, Biochim. Biophys. Acta 1255 (1995) 213–236.
[26] W. Curatolo, Thermal behavior of fractionated and unfractionated bovine brain cerebrosides, Biochemistry 21 (1982) 1761–1764.
[27] E. Freire, D. Bach, M.C. Correa-Freire, I. Miller, Y. Barenholz, Calorimetric investigation of the complex phase behavior of glucocerebroside dispersion, Biochemistry 19 (1980) 3662–3665.
[28] M.J. Ruocco, D. Atkinson, D.M. Small, R.P. Skarjune, E. Oldfield, G.G. Shipley, X-ray diffraction and calorimetric study of anhydrous and hydrated *N*-palmitoylgalactosylsphingosine (cerebroside), Biochemistry 20 (1981) 5957–5966.
[29] J.M. Boggs, K.M. Koshy, G. Rangaraj, Effect of fatty acid chain length, fatty acid hydroxylation, and various cations on phase behavior of synthetic cerebroside sulfate, Chem. Phys. Lipids 36 (1984) 65–89.
[30] I.R. Miller, D. Bach, Effect of ethylene glycol on the phase transition kinetics of gluco- and galactocerebrosides, Biochim. Biophys. Acta 863 (1986) 121–127.
[31] D.V. Lynch, M. Caffrey, J.L. Hogan, P.L. Steponkus, Calorimetric and X-ray diffraction studies of rye glucocerebroside mesomorphism, Biophys. J. 61 (1992) 1289–1300.
[32] K. Saxena, R.I. Duclos, P. Zimmermann, R.R. Schmidt, G.G. Shipley, Structure and properties of totally synthetic galacto- and gluco-cerebrosides, J. Lipid Res. 40 (1999) 839–849.
[33] D.C. Lee, I.R. Miller, D. Chapman, An infrared spectroscopic study of metastable and stable forms of hydrated cerebroside bilayers, Biochim. Biophys. Acta 859 (1986) 266–270.
[34] M. Bou Khalil, D. Carrier, P.T.T. Wong, N. Tanphaichitr, Polymorphic phases of galactocerebrosides: spectroscopic evidence of lamellar crystalline structures, Biochim. Biophys. Acta 1512 (2001) 158–170.
[35] W. Curatolo, L.J. Neuringer, The effects of cerebrosides on model membrane shape, J. Biol. Chem. 261 (1986) 17177–17182.
[36] M. Naito, K. Takahashi, H. Hojo, An ultrastructural and experimental study on the development of tubular structures in the lysosomes of Gaucher cells, Lab. Invest. 58 (1988) 590–598.
[37] W.J. Goux, H. Smith, D.R. Sparkman, Assembly of Alzheimer-like, insoluble filaments from brain cerebrosides, Neurosci. Lett. 192 (1995) 149–152.
[38] V.S. Kulkarni, W.H. Anderson, R.E. Brown, Bilayer nanotubes and helical ribbons formed by hydrated galactosylceramides: acyl chain and headgroup effects, Biophys. J. 69 (1995) 1976–1986.
[39] V.S. Kulkarni, J.M. Boggs, R.E. Brown, Modulation of nanotube formation by structural modifications of sphingolipids, Biophys. J. 77 (1999) 319–330.
[40] B. Ohler, I. Revenko, C. Husted, Atomic force microscopy of non-hydroxy galactocerebroside nanotubes and their self-assembly at the air–water interface, with applications to myelin, J. Struct. Biol. 133 (2001) 1–9.
[41] D.D. Archibald, P. Yager, Microstructural polymorphism in bovine

brain galactocerebroside and its two major subfractions, Biochemistry 31 (1992) 9045–9055.
[42] A.S. Goldstein, A.N. Lukyanov, P.A. Carlson, P. Yager, M.H. Gelb, Formation of high-axial-ratio-microstructures from natural and synthetic sphingolipids, Chem. Phys. Lipids 88 (1997) 21–36.
[43] D.D. Archibald, S. Mann, Self-assembled microstructures from 1,2-ethanediol suspensions of pure and binary mixtures of neutral and acidic biological galactosylceramides, Chem. Phys. Lipids 69 (1994) 51–64.
[44] P.R. Griffiths, G.L. Pariente, Introduction to spectral deconvolution, Trends Anal. Chem. 5 (1986) 209–215.
[45] D.G. Cameron, J.K. Kauppinen, D.J. Moffat, H.H. Mantsch, Precision in condensed phase vibrational spectroscopy, Appl. Spectrosc. 36 (1982) 245–250.
[46] J.M. Boggs, K.M. Koshy, G. Rangaraj, Influence of structural modifications on the phase behavior of semi-synthetic cerebroside sulfate, Biochim. Biophys. Acta 938 (1988) 361–372.
[47] A. Blume, W. Hubner, G. Messner, Fourier Transform infrared Spectroscopy of $^{13}C=O$ labeled phospholipids hydrogen-bonding to carbonyl groups, Biochemistry 27 (1988) 8239–8249.
[48] R.N.A.H. Lewis, D.A. Mannock, R.N. McElhaney, P.T.T. Wong, H.H. Mantsch, Physical properties of glycosyldiacylglycerols: an infrared spectroscopic study of the gel-phase polymorphism of 1,2-di-*O*-acyl-3-*O*-(β-D-glucopyranosyl)-*sn*-glycerols, Biochemistry 29 (1990) 8933–8943.
[49] E. Mueller, A. Blume, FTIR spectroscopic analysis of the amide and acid bands of ganglioside GM_1, in pure form and in mixtures with DMPC, Biochim. Biophys. Acta 1146 (1993) 45–51.
[50] A. Nabet, J.M. Boggs, M. Pézolet, Study by infrared spectroscopy of the interdigitation of C26:0 cerebroside sulfate into phosphatidylcholine bilayers, Biochemistry 35 (1996) 6674–6683.
[51] A. Menikh, P.-G. Nyholm, J.M. Boggs, Characterization of the interaction of Ca^{2+} with hydroxy and non-hydroxy fatty acids species of cerebroside sulfate by Fourier transform infrared spectroscopy and molecular modeling, Biochemistry 36 (1997) 3438–3447.
[52] K.M. Koshy, J.M. Boggs, Partial synthesis and physical properties of cerebroside sulfate containing palmitic acid or a-hydroxy palmitic acid, Chem. Phys. Lipids 34 (1983) 41–53.
[53] M.C. Sullards, D.V. Lynch, A.H. Merrill, J. Adams, Structure determination of soybean and wheat glucosylceramides by tandem mass spectrometry, J. Mass Spectrom. 35 (2000) 347–353.
[54] D.J. Moore, M.E. Rerek, R. Mendelsohn, FTIR spectroscopy studies of the conformational order and phase behavior of ceramides, J. Phys. Chem., B 101 (1997) 8933–8940.
[55] I. Pascher, S. Sundell, Molecular arrangements in sphingolipids. The crystal structure of cerebroside, Chem. Phys. Lipids 20 (1977) 175–191.
[56] H.L. Casal, H.H. Mantsch, Polymorphic phase behavior of phospholipid membranes studies by infrared spectroscopy, Biochim. Biophys. Acta 779 (1984) 381–401.
[57] M.C. Correa-Freire, E. Freire, Y. Barenholz, R.L. Biltonen, T.E. Thompson, Thermotropic behavior of monoglucocerebroside-dipalmitoylphosphatidylcholine multilamellar liposomes, Biochemistry 18 (1979) 442–445.
[58] J.M. Schnur, B.R. Ratna, J.V. Selinger, A. Singh, G. Jyothi, K.R.K. Easwaran, Diacetylenic lipid tubules: experimental evidence for a chiral molecular architecture, Science 264 (1994) 945–947.
[59] P. Yager, P.E. Schoen, Formation of tubules by a polymerizable surfactant, Mol. Cryst. Liq. Cryst. 106 (1984) 371–381.
[60] K. Saxena, R.I. Duclos Jr., P.K. Sripada, G.G. Shipley, Unusual hydration properties of C16:0 sulfatide bilayer membranes, Biophys. J. 79 (2000) 385–393.
[61] R. Skarjune, E. Oldfield, Physical studies of cell surface and cell membrane structure. Deuterium magnetic resonance studies of *N*-palmitoylglucosylceramide (cerebroside) head group structure, Biochemistry 21 (1982) 3154–3160.